Centre for Pharmaceutical Research[1], School of Pharmaceutical, Molecular and Biomedical Sciences, University of South Australia, and School of Pharmacy[2], The University of Auckland, New Zealand

Prediction of corneal permeability using artificial neural networks

S. Agatonovic-Kustrin[1], A. Evans[1], R. G. Alany[2]

Received March 03, 2003, accepted March 10, 2003

Dr. Raid G. Alany, School of Pharmacy, The University of Auckland, 85 Park Road Grafton, Private Bag 92019, Auckland 1, New Zealand
r.alany@auckland.ac.nz

Pharmazie 58: 725–729 (2003)

The purpose of this study was to develop a simple model for prediction of corneal permeability of structurally different drugs as a function of calculated molecular descriptors using artificial neural networks. A set of 45 compounds with experimentally derived values of corneal permeability (log C) was used to develop, test and validate a predictive model. Each compound was encoded with 1194 calculated molecular structure descriptors. A genetic algorithm was used to select a subset of descriptors that best describe corneal permeability coefficient log C and a supervised network with radial basis transfer function (RBF) was used to correlate calculated molecular descriptors with experimentally derived measures of corneal permeability. The best model, with 4 input descriptors and 12 hidden neurones was chosen, and the significance of the selected descriptors to corneal permeability was examined. Strong correlation of predicted with experimentally derived log C values (correlation coefficient greater than 0.87 and 0.83 respectively) was obtained for the training and testing data sets. The developed model could be useful for the rapid prediction of the corneal permeability of candidate drugs based on molecular structure alone as it does not require experimentally derived data.

1. Introduction

The cornea is one of the major pathways for penetration into the eye of topically applied drugs [1]. It acts as a protective barrier to invasion of foreign substances and also as a barrier to drug transport. On the other hand, the conjunctiva and sclera are more permeable than the cornea [2–4], but then the blood circulation tends to remove the drug before it can enter the inner ocular tissues. For this reason, a large number of experimental work was performed to characterise corneal permeability and different models have been developed [5–7].

Lipophilicity of the drug seems to be the most important property. The cornea is composed of five layers (Fig. 1),

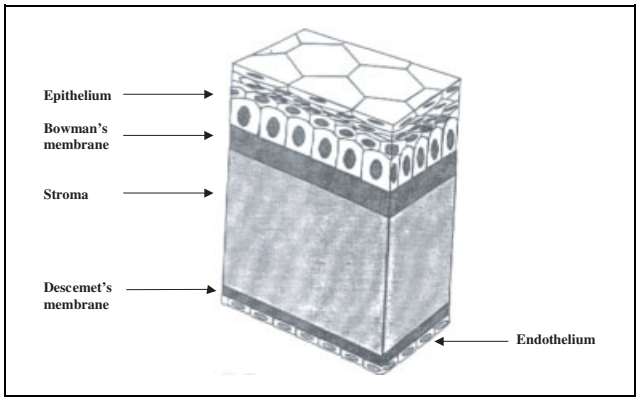

Fig. 1: Schematic illustration of the cornea, showing the comprising five layers [47].

the epithelium and stroma being the most significant for drug delivery [8]. The rate-limiting barrier for hydrophilic drugs is the lipophilic corneal epithelium, while for lipophilic drugs the aqueous stroma is the major barrier. Few models have been developed to predict corneal permeability as a function of the partition coefficient or the distribution coefficient of the drug [9, 10] and both a parabolic [11] and a sigmoidal [12] relationship have been shown to describe the influence of drug lipophilicity on corneal drug penetration. However, these models are applicable only to structurally related compounds. In addition to the lipophilicity of a drug, its aqueous solubility [13], molecular size [14], charge [15] and degree of ionisation [16, 17] also affect corneal absorption. Tear fluid has limited buffering capacity [18].

Thus, the pH and buffering capacity of the instilled solution affect the pH of tear fluid [19, 20] and drug ionisation in the pre-corneal area, hence drug absorption. The un-ionised form of the drug penetrates the cornea more easily than the ionised form [21] and, thus, the pH and buffering capacity of the instilled solution can have a significant effect on ophthalmic drug absorption. Yoshida and Topliss [22] developed a model based on octanol-water partition coefficient (log P), the alkane-water partition coefficient (Δ log P) and the distribution coefficient (log D) as predictors. However, Δ log P values are usually difficult to obtain. For example triamcinolone acetonide, prednisolone acetate, dexamethasone acetate, and timolol could not be included in their QSAR (quantitative structure-activity relationship) studies because of a lack of Δ log P values. Therefore, it would be useful to predict

corneal permeabilities of miscellaneous compounds from calculated parameters derived only from a molecular structure if experimental data are not available. This is of particular interest in cases, where the relevant property is difficult to measure, or where the compound itself is not available.

Among the novel *in silico* prediction models that are finding increased application in pharmaceutical research are artificial neural networks (ANN). An ANN is a biologically inspired computer program designed to simulate the way in which the human brain processes information. It gathers its knowledge by detecting the patterns and relationships in data and learns (or is trained) through experience with appropriate learning exemples, not from programming. The potential applications of ANN methodo-logy in the pharmaceutical sciences are broad. They range from interpretation of analytical data (modelling the pharmaceutical analysis in quality control), drug design (molecular modelling) and dosage form design (optimization of manufacturing processes) to clinical pharmacy through biopharmacy (pharmacokinetic and pharmacodynamic modelling) (Agatonovic-Kustrin and Beresford 2000) [23]. The use of ANNs in a biological activity prediction is a new but expanding area in the field of pharmaceutical research.

In this paper, we report on a simple four parametric Quantitative Structure Permeability Relationship QSPR model that was developed and applied to structurally non-related compounds. An ANN was used to correlate molecular descriptors with corneal permeability and optimize the model.

2. Investigations, results and discussion

The first step in developing the QSPR model was to calculate numerical descriptors. A total of 1194 descriptors divided in 16 classes were calculated (Table 1). Log C values were used as the ANN's output and calculated molecular descriptors as the inputs. Initially ANN models consisting of 1194 inputs (molecular descriptors), one hidden layer and one output neuron (target, log C) with different topology and transfer function were trained and tested. The number of inputs and hidden neurons were optimised during this early phase of training. The next step was to determine which of the available input variables [24] should be used to build the ANN model (variable selection). Selection of the important molecular descriptors and examination of the variable contribution to the model through output sensitivity is an important aspect of a QSPR study, not only for ranking the relative importance of each variable and calculating its statistical significance, but also as a mean of refining the model by variable selection.

Table 1: Calculated molecular descriptors

Topological descriptors	226
Molecular walk counts	19
BCUT descriptors	64
2D autocorrelations	96
Aromaticity indices	4
Randic molecular profiles	41
Geometrical descriptors	31
RDF descriptors	150
3D-MoRSE descriptors	160
WHIM[a] descriptors	99
GETAWAY[b] descriptors	197
Functional groups	25
ACF[c] descriptors	39
Empirical descriptors	3
Properties	3
Constitutional descriptors	37
total	1194

[a] WHIM (Weighted Holistic Invariant Molecular descriptors)
[b] GETAWAY (GEometry, Topology and Atoms-Weighted Assembly)
[c] Atom centre fragments descriptor (ACF)

Neural networks are much more complex models than the linear techniques used in conventional modelling. They are more difficult to optimize, and there are difficult design decisions to make, such as the right type and complexity of network for the problem, and the right input variables to use. Large numbers of input variables cause overtraining of data resulting in models with a poor ability to generalize. Some neural network architectures (e.g., MLP) can actually learn to ignore useless variables.

However, other architectures (e.g., RBF) are adversely affected with useless variables. In all cases a larger number of inputs implies that a larger number of training cases is required to prevent over-learning. As a rule of thumb, the number of training cases should be at least few times bigger than the number of weights in the network. As a consequence, the performance of a network could be improved by reducing the number of inputs, even sometimes at the cost of losing some input information. For that reason, the sensitivity analysis on the inputs to a neural network was performed. Input variables are not, in general, independent, that is there are interdependencies between variables.

Sensitivity analysis rates variables according to the deterioration in modelling performance that occurs if that variable is no longer available to the model. It assigns a single rating value to each variable. Sensitivity was used to identify key inputs that are always of high sensitivity and others that are always of low sensitivity, and "ambiguous" inputs that change ratings and probably carry mutually redundant information. Best models were selected to perform sensitivity and to examine the activation level (outputs) of the input neurons.

Inputs whose average activation was equal to zero with low sensitivity and with variable sensitivity were eliminated from the network. Following this procedure the number of inputs was reduced to 4 inputs only. As expected this reduced the size and complexity of the network and thus training time, and improved the network performance.

The RBF model with 4 input descriptors (polar surface area, global shape index unweighted (Ku), global shape index weighted by atomic Sanderson electro negativities (Ke), oxygen atom of the carbonyl group was found to have the best predictive performance. The model had one hidden layer with 12 neurons, thus producing a 4-12-1 architecture. Drug penetration through the biological membranes depends upon a number of molecular properties, such as lipophilicity, polarity, degree of ionization and molecular size. Physicochemical factors that affect corneal permeability include the intrinsic solubility of the drug molecule and its membrane permeability. The model confirms that, for a given drug, these properties are in turn determined by its molecular size, shape and polarity.

The octanol-water partition coefficient (log P) is frequently used in quantitative structure-activity relationships [25] as a measure of the lipophilic character of the molecules. Lipophilicity is approximately correlated to passive transport across cell membranes and the ability of a compound to partition through a membrane [26]. Correlations of lipo-

philicity and membrane penetration have been extensively reviewed by Seydel and Schaper [27], and the role of lipophilicity has also been the subject of some recent work [28].

The octanol-water partition coefficient (log P) is well established as a key parameter to describe lipophilicity, uptake and distribution in biological systems. It is frequently used in quantitative structure-activity/property relationships [29–31]. However, log P is a ratio [32] and a compound with low solubility in both octanol and water could have the same log P as a compound with 100 times higher solubility in both solvents. It follows that calculated log P could only be roughly correlated with corneal permeability for a homologous series of compounds [33], as it does not account for intramolecular interactions.

For example, intramolecular hydrogen bonding [34] can dramatically influence absorption properties. It follows that other descriptors must also be taken into account.

This study has shown that polar surface area (PSA) and hydrogen bonding capacity plays a significant role in the description of drug membrane penetration [35–37]. The utility of polar surface area as a predictor of absorption has even been previously identified [38]. Molecular surface area and molar volume are highly correlated geometrical descriptors that can provide information about contact surface, surface diffusion, absorption and information of the size of the molecules. The contact surface area can be viewed as an indicator of the extent to which the solute is exposed to intermolecular interaction with the solvent [39] and is shown to be a remarkably accurate predictor of water solubility [40]. Drugs need to be in solution to penetrate biological membranes. Therefore, as a general rule, a drug that is very poorly soluble or insoluble in water would have variable or unreliable corneal permeability. The increase in PSA will increase corneal permeability perhaps due to increase in aqueous solubility.

In addition, hydrogen bonds are major forces of molecular recognition and an essential component of intermolecular interactions. The polar surface area is also an indication of a compound's capacity to form hydrogen bonds. Higher log C values are observed for compounds with higher PSA. Calculated surface characteristics correlate with a number of physical-chemical properties of drug molecules including lipophilicity, the energy of hydration and the hydrogen bond formation capacity [41, 42]. The surface properties of a molecule that forms an intramolecular hydrogen bond may be less polar resulting in enhanced membrane permeability in comparison to a homologous molecule that exposes the (polar) hydrogen-bonding group on its surface. In that sense, we can assume that the polar molecular surface area reflects intramolecular hydrogen bonding.

WHIM (Weighted Holistic Invariant Molecular descriptors) and GETAWAY (GEometry, Topology and Atoms-Weighted AssemblY) are 3-dimensional molecular descriptors recently developed [43]. WHIM descriptors contain chemical information concerning size, geometry, shape and contribution of the molecule atoms. They are based upon atomic contributions to van der Waals surface area, log P, molar refractivity and partial charge. WHIM descriptors are 3-dimensional descriptors based on the calculation of key component axes calculated from a weighted covariance matrix obtained by the molecule geometrical coordinates. Six different weighted methods are used for the weighted covariance matrix: u (unweighted), m (atomic mases), p (atomic polarizability), v (van der Waals volume), e (atomic electronegativity) and s (atomic electrotopological state). The developed model included unweighted global shape index and global shape index weighted by with atomic electronegativity as a measure of molecular size and polarity.

The last descriptor that was included in the model is the oxygen of the carbonyl group, an atom center fragments descriptor (ACF) [44]. Every non-hydrogen atom forms the basis of an ACF descriptor. ACF classification system was developed by declaring different types for atoms with different nearest neighbors. For instance, the first carbon of CH_3C is treated as different from that of CH_3N. More precisely, every ACF is characterized by the atom type of its central atom, by the types of all directly connected (neighbour) atoms, by the types of the respective chemical bonds, and by the number of directly attached hydrogen atoms.

Characterization of the atom type includes aromaticity and may also include formal atomic charge and number of unpaired electrons. To account for molecular size effects, molar mass is added as a formal ACF. The final atom classification system in this study generated 39 basic atom type descriptors. The developed model has identified the oxygen atom of the aromatic carbonyl group as common biophore.

The resulting model could be explained with reference to the corneal anatomy (Fig. 1). The cornea contains three primary layers: epithelium, stroma, and endothelium. Both the epithelium and the endothelium are lipophilic and provide main barriers to hydrophilic compounds. The stroma is an aqueous layer and limits the movement of lipophilic compounds across the cornea. Therefore, a compound usually has greater corneal permeability when it has adequate hydrophilic groups and adequate size. In general, the penetration of a compound through biological membranes decreases as its molecular size increases [45].

The interpretation of effects of individual descriptors is difficult as the model is multivariate and non-linear. However, some insight into the degree of non-linear behaviour of selected descriptors could be obtained with a functional dependence plot. The value of input variables is varied through its range, while all other inputs are held constant. The network output is plotted against variable descriptors to generate a functional dependence plot. This gives an idea of how the network output alters in response to the selected input. Fig. 2 displays functional dependence surfaces of selected descriptors. The observed non-linearity of the un-weighted shape indices and ACF for the carbonyl oxygen inputs is clear evidence on the complex relationship between these descriptors and log C values. As expected, the molecular size (PSA and shape indices) displays a negative dependence on the corneal permeability. It is very interesting that methanol fits well to the model. Methanol is a very small hydrophilic compound. It was considered that methanol penetrates across the cornea by an aqueous 'pore' pathway and was usually underestimated by other model [46].

As part of evaluating the quality of the developed model strong correlation of predicted vs. experimentally derived log C values (correlation coefficient greater than 0.87 and 0.83 respectively) was obtained for the training and testing data sets (Table 2). The fact that the slope value was not significantly different from the unity indicated minimal or almost no proportional error and as the intercept was not different from zero reflected no method bias. To further assess and validate the predictive ability of the model we predicted the log C values of eight compounds outside the training set (Table 3).

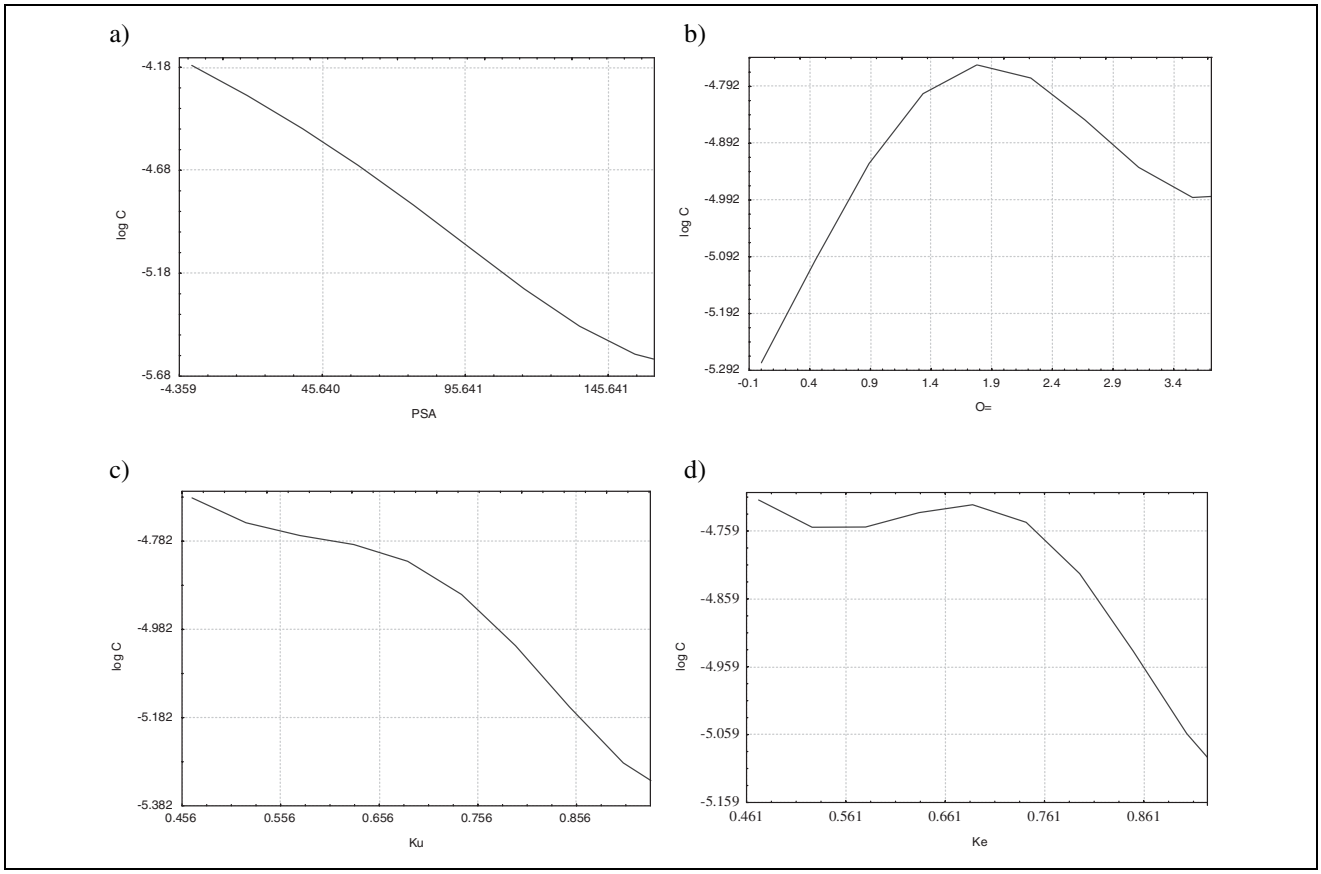

Fig. 2: Functional dependence plots of the four most significant descriptors from the final model. The descriptors are a) Polar Surface Area (PSA); b) Carbonyl group oxygen (O=); c) Un-weighted global shape index (Ku); d) Global shape index weighted by atomic Sanderson electronegativity (Ke).

The results in Table 3 show that calculated log C values agreed reasonably well with their experimentally determined counterparts. However, it should be pointed out that this model was focused on predicting the corneal permeability of candidate drugs based solely on their molecular structure without taking into account processes that normally precedes corneal absorption such as dilution by resident tears, tear turnover, interaction with the pre-corneal tear film, nasolacrimal drainage, drug protein binding, drug metabolism and non-productive absorption, a limitation that will hopefully be addressed in future work.

In condusion, it can be stated that a simple model for corneal permeability prediction was developed. The model components were derived from the molecular structure of diverse compounds and contained descriptors, which could be easily calculated as independent variables. It is a simple model that could serve as a useful screening tool for newly developed molecules that are intended for topical application to the surface of the eye and are expected to traverse the corneal barrier.

Table 2: Regression statistics of the 4-12-1 RBF model

	Training	Testing	Validation
Data Mean	−4.84	−5.05	−4.89
Data S. D.	0.60	0.77	0.82
Error mean	−0.19	−0.11	0.06
Error S. D.	0.30	0.45	0.78
Abs E. mean	0.30	0.40	0.61
S. D. ratio	0.50	0.58	0.95
Correlation	0.87	0.83	0.85

S. D. = Standard deviation

3. Experimental

3.1. Software

Statistica Neural Network 4.0 F (StatSoft Inc., Tulsa, USA) was used for building the QSAR and Dragon 2.1 (Milano Chemometric and QSAR Research Group, Milano, Italy) was used to calculate molecular descriptors from the molecular structure.

3.2. Data collection and manipulation

A set of 45 structurally different compounds and their experimentally derived corneal permeability coefficient values (log C) were collected from the literature. For each of the 45 drug molecules, 1194 descriptors were calculated (Table 1). Log C values were used as the ANN's output and calculated molecular descriptors as the inputs. The collected data set was split into three subsets: training (30 data sets), testing (8 data sets) and validation (7 data sets). The results of five runs were averaged. During training, the performance of the ANN was evaluated with testing data. The training set was used to train the network and the testing set was used to monitor performance and overtraining. Training was stopped when the training root mean squared error (RMS) failed to improve over a given number of training cycles and when the testing RMS error started to increase. Validation set was used later to evaluate the trained model.

3.3. ANN Models for corneal permeability prediction

ANNs are constituted from hundreds of single processing elements (PE), or so called artificial neurons. Each PE has weighted inputs, transfer function and one output. PEs are connected with coefficients (weights) which constitute the neural structure and are organised in layers, the input layer, the output layer, and the hidden layers between them. The input layer neurons receive data from a data file. The output neurons provide the ANN's response to the input data. The weighted sum of the inputs composes the activation of the neuron. The activation signal is passed through an activation function (also known as a transfer function) to produce a single output of the neuron. Thus, the hidden layer is where the network learns interdependencies in the model and transfer functions for the hidden units introduces nonlinearity into the network.

Multilayer perceptrons (MLPs) and radial basis function (RBF) networks are the two most commonly used types of feed-forward network. The main

Table 3: Model performance in the prediction of log C values; predicted and measured [48–51] corneal permeability coefficients

Compound	Log C[c]		Residual	RMS
	Predicted	Measured	error	error
4-Chlorobenzen-sulfonamide	−4.75	−4.26	−0.50	1.37
4-Chloro-methyl-benzensulfonamide[b]	−4.61	−4.19	−0.42	1.16
Acebutolol	−6.18	−6.06	−0.12	0.34
Acetazolamide	−6.37	−6.24	−0.13	0.37
Alprenolol	−4.79	−4.54	−0.25	0.70
Atenolol[a]	−5.68	−6.17	0.49	1.35
Betaxolol[a]	−4.98	−4.57	−0.42	1.15
Bevantalol	−4.85	−4.24	−0.61	1.69
Bufuralol[b]	−4.83	−4.14	−0.70	1.92
Butanol	−4.59	−4.12	−0.48	1.32
Chloramphenicol	−5.31	−5.17	−0.14	0.40
Clonidine	−4.45	−4.36	−0.10	0.27
Cortexolone	−5.10	−4.52	−0.59	1.61
Cromolyn[a]	−5.79	−5.97	0.18	0.49
Cyclophosphamide[a]	−4.43	−4.95	0.51	1.41
Desoxycorticosterone	−4.98	−4.40	−0.59	1.61
Dexamethasone	−4.97	−5.30	0.33	0.90
Dexamethasone acetate	−4.74	−4.43	−0.31	0.87
Fluorometholone	−4.81	−4.78	−0.04	0.10
Hydrocortisone	−5.06	−5.07	0.01	0.02
Ibuprofen	−4.77	−4.65	−0.12	0.33
Indomethacin	−4.64	−4.16	−0.48	1.33
Levobunolol	−4.60	−4.78	0.18	0.49
Methanol	−4.47	−4.04	−0.43	1.18
Methazolamide[a]	−5.67	−5.43	−0.25	0.69
Metoprolol[a]	−5.00	−4.63	−0.37	1.02
Nadolol[b]	−4.96	−6.00	1.04	2.86
Oxprenolol	−4.89	−4.60	−0.29	0.79
Penbutolol	−4.74	−4.35	−0.39	1.06
Phenylephrine[b]	−4.81	−6.03	1.22	3.37
Pilocarpine	−4.68	−4.77	0.09	0.25
Pindolol[b]	−4.90	−5.00	0.10	0.27
Prednisolone	−5.46	−5.43	−0.03	0.09
Prednisolone acetate[b]	−5.07	−4.48	−0.59	1.62
Progesterone	−5.21	−4.71	−0.50	1.38
Propranolol	−4.78	−4.32	−0.46	1.27
Rauwolfine	−4.98	−5.04	0.06	0.17
Sotalol	−5.26	−5.80	0.54	1.48
Sulfacetamide	−5.39	−5.72	0.33	0.92
Testosterone[b]	−4.59	−4.37	−0.22	0.61
Timolol[a]	−5.22	−4.91	−0.31	0.86
Triamcinolone	−5.31	−4.80	−0.51	1.40
Vidarabine	−6.02	−5.77	−0.25	0.70
Water[a]	−4.54	−3.82	−0.72	1.98
Yohimbine	−4.85	−4.75	−0.11	0.29

[a] testing data set
[b] validation data set
[c] C: (cm/s)

difference between the two is the way in which hidden units combine values coming from preceding layers in the network. An MLP models the response function using the composition of sigmoid and linear functions whereas a radial basis function network (RBF) has a hidden layer of radial units, each modelling a Gaussian response surface, peaked at the centre, and descending outwards. Just as an MLP neurone responds (non-linearly) to the distance of points from the line of the sigmoid projection, in a radial basis function network neurones respond (non-linearly) to the distance of points from the centre. MLP units are defined by their weights and threshold, which together give the equation of the defining line. In contrast a radial unit is defined by its centre point and a radius. Therefore the number of centres, the positioning of the centres and the transfer function are the key factors affecting its performance and these factors were varied in the training process.

On a practical level RBF trains much faster and would be the best choice for predicting small sample data. In contrast, MLP has more potential in predicting more complex data as it has more than one layer of hidden neurons.

References

1 Doane, M. G.; Jensen, A. D.; Dohlman, C. H.: Am. J. Ophthalmol. **85**, 383 (1978)
2 Ahmed, I.; Gokhale, R. D.; Shah, M. V.; Patton, T. F.: J. Pharm. Sci. **76**, 583 (1987)
3 Wang, W.; Sasaki, H.; Chien, D. S.; Lee, V. H. L.: Curr. Eye Res. **10**, 571 (1991)
4 Ashton, P.; Podder, S. K.; Lee, V. H. L.: Pharm. Res. **8**, 1166 (1991)
5 Fu, X. C.; Liang, W. Q.: Pharmazie **56**, 667 (2001)
6 Fu, X. C.; Liang, W. Q.: Int. J. Pharm. **232**, 193 (2002)
7 Grass, G. M.; Robinson, J. R.: J. Pharm. Sci. **77**, 3 (1988)
8 Huang, H. S.; Schoenwald, R. D.; Lach, J. L.: J. Pharm. Sci. **72**, 1272 (1983)
9 Schoenwald, R. D.; Huang, H. S.: J. Pharm. Sci. **72**, 1266 (1983)
10 Schoenwald, R. D.; Ward, R. L.: J. Pharm. Sci. **67**, 786 (1978)
11 Chang, S. C.: Thesis. School of Pharmacy, University of Southern California, Los Angeles 1987
12 Wang, W.; Sasaki, H.; Chien, D. S.; Lee, V. H. L.: Curr. Eye Res. **10**, 571 (1991)
13 Sieg, J. W.; Robinson, J. R.: J. Pharm. Sci. **66**, 1222 (1977)
14 Liaw, J.; Robinson, J. R.: Int. J. Pharm. **88**, 125 (1992)
15 Liaw, J.; Rojanasakul, Y.; Robinson, J. R.: Int. J. Pharm. **88**, 111 (1992)
16 Maren, T. H.; Jankowska, L.: Curr. Eye Res. **4**, 399 (1985)
17 Brechue, W. F.; Maren, T. H.: Invest. Ophthalmol. Vis. Sci. **34**, 2581 (1993)
18 Carney, L. G.; Hill, R. M.: Arch. Ophthalmol. **97**, 951 (1979)
19 Longwell, A.; Birss, S.; Keller, N.; Moore, D.: J. Pharm. Sci. **65**, 1654 (1976)
20 Ahmed I.; Patton, T.: Int. J. Pharm. **19**, 215 (1984)
21 Benson, H.; Alto P.: Arch. Ophthalmol. **91**, 313 (1974)
22 Yoshida, F.; Topliss, J. G.: J. Pharm. Sci. **85**, 819 (1996)
23 Agatonovic-Kustrin, S.; Beresford, R.: J. Pharm. Biom. Anal. **22**, 717 (2000)
24 Reed, R.: IEEE T. Neural Network **4**, 740 (1993)
25 Dearden, J. C.: Environ. Health Perspect. **61**, 203 (1985)
26 Brodie, B. B.; Hogen, C. A. M.: J. Pharmacol. **3**, 345 (1957)
27 Seydel, J. K.; Schaper, K. J.: Pharmacol. Ther. **15**, 131 (1981)
28 Escribano, E.; Calpena, A. C.; Garrigues, T. M.; Freixas, J.; Domenech, J.; Moreno, J.: Antimicrob. Agents Chemother. **41**, 1996 (1997)
29 Dearden, J. C.: Environ. Health Perspect. **61**, 203 (1985)
30 Famini, G. R.; Penski, C. A.: J. Phys. Org. Chem. **5**, 395 (1992)
31 Heaberlein, M.; Brinck, T.: J. Chem. Soc. Perkin Trans. **2**, 289 (1997)
32 Egan, W. J.; Merz, K. M. Jr.; Baldwin, J. J.: J. med. Chem. **43**, 3867 (2000)
33 Schoenwald, R. D.; Ward, R. L.: J. Pharm. Sci. **67**, 786 (1978)
34 Norinder, U.; Osterberg, T.; Artursson, P.: Eur. J. Pharm. Sci. **8**, 49 (1999)
35 Clark, D. E.: J. Pharm. Sci. **88**, 807 (1999)
36 Abraham, M. H.; Martins, F.; Mitchell, R. C.: J. Pharm. Pharmacol. **49**, 858 (1997)
37 Winiwarter, S.; Ax, N. M.; Bonham, F.; Hallberg, A.; Lennernas, H.; Karlen A.: J. Med. Chem. **41**, 4939 (1998)
38 Palm, K.; Stenberg, P.; Luthman, K.; Artursson, P.: Pharm. Res. **14**, 568 (1997)
39 Hermann, R. B.: J. Comput. Chem. **18**, 115 (1997)
40 Bodor, N.; Huang, M. J.: J. Pharm. Sci. **81**, 954 (1992)
41 Ooi, T.; Oobatake, M.; Némethy, G.; Scheraga H. A.: Proceedings of the National Academy of Science USA (1987)
42 Dunn, W. J. III; Koehler, M. G.; Grigoras, S.: J. Med. Chem. **30**, 1121 (1987)
43 Todeschini, R.; Lasagni, R.; Marengo, E.: J. Chemometrics **8**, 263 (1994)
44 Wildman, S. A.; Crippen, G. M.: J. Chem. Inf. Comput. Sci. **39**, 868 (1999)
45 Van de Waterbeemd, H.; Camenish, G.; Folkers, G.; Raevsky, O. A.: Quant. Struct. Act. Relat. **15**, 480 (1996)
46 Grass, G. M.; Robinson, J. R.: J. Pharm. Sci. **77**, 3 (1988)
47 Sasaki, H.; Yamamura, K.; Mukai, T.; Nishida, K.; Nakamura, J.; Nakashima, M.; Ichikawa, M.: Critical Reviews in Therapeutic Drug Carrier Systems **16**, 85 (1999)
48 Edwards, A.; Prausnitz, M. R.: Pharm. Res. **18**, 1497 (2001)
49 Huang, H. S.; Schoenwald, R. D.; Lach, J. L.: J. Pharm. Sci. **72**, 1272 (1983)
50 Yoshida, F.; Topliss, J. G.: J. Pharm. Sci. **85**, 819 (1996)
51 Muchtar, S.; Abdulrazik, M.; Frucht-Pery, J.; Benita, S.: J. Control. Rel. **44**, 55 (1997)